DISCLAIMER

CASL-U-2019-2018-000

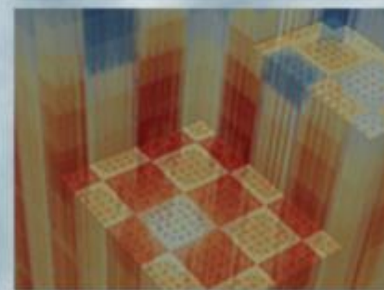

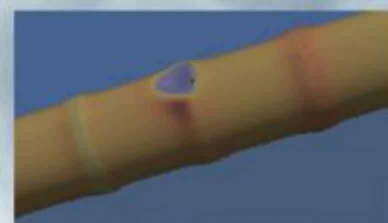

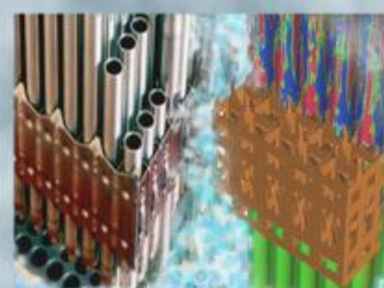

Modeling the Ex-core Detector Response into a Production Option in MPACT

Yuxuan Liu, University of Michigan

Eva Davidson, Oak Ridge National Laboratory

05/31/2019

REVISION LOG

Revision	Date	Affected Pages	Revision Description
0	05/31/19	All	Initial Release

Document pages that are:

Export Controlled ____________No____

IP/Proprietary/NDA Controlled___No____________________________________

Sensitive Controlled______________No___________________________________

Requested Distribution:

To:

Copy:

EXECUTIVE SUMMARY

In the past few years, the Consortium for Advanced Simulation of Light Water Reactors (CASL) has overseen a successful activity to extend the radiation transport capability from the reactor in-core geometry to the ex-core geometry by coupling the deterministic neutronics code MPACT, with the Monte Carlo code Shift. However, transient problems such as RIAs require an efficient prediction of the ex-core detector response to determine the timeframe for a reactor trip. Therefore, in addition to the high-fidelity MPACT-Shift coupled calculation, separate efforts have been made to explore simplified methods for ex-core detector response with MPACT standalone calculation.

In a previous milestone L3_RTM.MCH.P17.06, several simplified methods for ex-core detector response were developed in MPACT. In particular, the double kernel method is based on the default MPACT core geometry, so extensive modeling or transport calculation with full reflector and ex-core details are not needed in this method. Since the 1-D diffusion and neutron streaming kernels are used for extended ex-core calculations, the extra computational efforts are very small.

The work implemented in the current milestone provides a fully integrated option for MPACT to approximately calculate the ex-core detector response using the double kernel method. To overcome the difficulty of obtaining the consistent diffusion coefficients (these were obtained through separate CMFD calculation and edits), the 1-D diffusion solver is replaced by a 1-D Sn transport solver to compute the neutron flux at the vessel outer surface. The new VERA inputs for ex-core detector are processed in MPACT. The detector signals are linked to the SCRAM logic as an option to trip the core during transient calculation. Two sets of 3-D quarter core problems are run with MPACT standalone and VeraShift to verify the radial and axial effects on detector response by varying the moderator density and control rod position. For the cases with moderator density changes, the detector responses from MPACT are within 2 sigma error of VeraShift. For the cases at different control rod positions, the axial offsets computed from MPACT are within 2% error of VeraShift results.

CONTENTS

FIGURES

TABLES

ACRONYMS

AMA	Advanced Modeling Applications
BWR	boiling water reactor
CASL	Consortium for Advanced Simulation of Light Water Reactors
CZP	Cold Zero Power
HZP	Hot Zero Power
BOL	Beginning of Life
EOL	End of Life
OLCF	Oak Ridge Leadership Computing Facility
ORNL	Oak Ridge National Laboratory
PWR	pressurized water reactor
RIA	reactivity insertion accident
RPV	reactor pressure vessel
RTM	Radiation Transport Methods
V&V	verification and validation
VERA	Virtual Environment for Reactor Applications

1. INTRODUCTION

The Consortium for Advanced Simulation of Light Water Reactors (CASL) Virtual Environment for Reactor Applications (VERA) [1] offers unique capabilities for high-fidelity neutron transport within the reactor core geometry. Recent developments [2,3] have extended the transport capability to the ex-core geometry by coupling the deterministic neutronics code MPACT [4], with the Monte Carlo code Shift [5]. Specifically, MPACT solves steady-state or transient problems and passes the fission source to Shift for a follow-on fixed source transport calculation with full details of the ex-core geometry. One of our interests in the ex-core transport applications is the ex-core detector response. For instance, the power range detectors are routinely used to monitor the core-average power distribution during the reactor operation and transient scenarios. The MPACT (in-core) and Shift (ex-core) coupled calculation has been successful in predicting the ex-core detector response [3]. However, additional computing time and memory usage are anticipated for the coupled calculation as compared to the standalone MPACT transport calculation.

In the previous milestone L3_RTM.MCH.P17.06, we investigated several simplified methods for ex-core detector response with standalone MPACT [6]. Three methods based on MPACT capabilities are developed for efficient calculation of the ex-core detector response, and are verified with MPACT-Shift coupled calculation. In particular, the double kernel method is based on the default MPACT core geometry, so extensive modeling or transport calculation with full reflector and ex-core details are not needed in this method.

The work implemented in the current milestone provides a fully integrated option for MPACT to approximately calculate the ex-core detector response using the double kernel method. To overcome the difficulty of obtaining the consistent diffusion coefficients, which were previously obtained through separate CMFD calculation and edits, the 1-D diffusion solver is replaced by a 1-D Sn transport solver to compute the neutron flux at the vessel outer surface. The new VERA inputs for ex-core detector are processed in MPACT. The detector signals are linked to the SCRAM logic as an alternative option to trip the core during transient calculation.

2. DESCRIPTION OF IMPLEMENTATION

Ex-core neutron flux monitoring system (i.e., ex-core neutron detectors) is routinely used to monitor the core-average power distribution through the neutron leakage out of the reactor vessel. In PWRs, the ex-core detector is typically installed in the reactor cavity area located outside the reactor pressure vessel, as shown in Fig. 1. These detectors generally use neutron reactions to produce charged particles for detection signals (BF_3 gas detector, boron coated ion chamber, or U-235 fission chamber) [7]. The detector response R can be written as,

$$R = < \Sigma_D \phi > \tag{1}$$

where Σ_D is the detector response function that corresponds to the cross section of the detector material, ϕ is the neutron flux, and $< \cdot >$ denotes integration over angle, energy and space of the continuous domains within a detector.

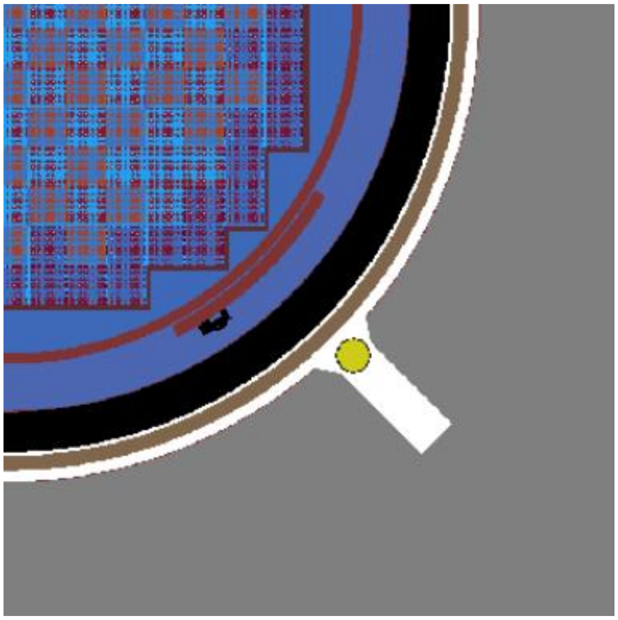

Figure 1 A Power range detector based on Watts Bar 1

The geometry modeling capability in MPACT was originally designed for in-core configurations. Because of the irregularity of the ex-core geometry (detector subtleties, surveillance capsule, concrete cavity, etc.), modeling the ex-core geometry exactly with MPACT would require a lot more work for the additional geometrical complexity. Also, MPACT uses the 2D/1D method with a 3D CMFD calculation to accelerate the solution. Solving the full geometry with ex-core components would significantly increase the computing time, and more importantly, may cause stability issues of the CMFD because of the void region outside the reactor vessel. Therefore, several simplified methods were developed in the previous milestone based on low-order methods and reduced geometrical configurations [6].

In the current milestone, the double kernel method is improved by replacing the analytic diffusion solver with Sn solver to overcome the difficulty of obtaining the consistent diffusion coefficients. The input processing and the usage of detector signal for SCRAM are implemented to enable a production option of the ex-core detector response into MPACT.

2.1 Double Kernel Method

Instead of solving the transport equation up to the ex-core detector, point kernels can be used to compute the flux in detector by integrating the sources over the whole geometry. Conventional kernel methods use empirical point kernels, where the attenuation cross sections from fission sources to detector were chosen to fit experimental data for thermal neutron flux in water [8]. Improved kernel method also takes into account the vessel scattering effect [9], but the vessel neutron sources are still evaluated by empirical point kernels. In MPACT, axial and radial reflectors are explicitly modeled, so the neutron leakage out of the reflector can be explicitly estimated. Therefore, point kernels can be used between the transport solution boundary of MPACT and the ex-core detector.

2.1.1 Neutron Streaming Kernel

The left configuration in Fig. 2 shows a simplified ex-core geometry that MPACT uses to model the ex-core detector. Compared to Fig. 1, the cavity in the concrete is neglected and the concrete thickness is reduced. By doing this, we assume the effect of neutrons scattering back from the concrete could be approximated by a constant factor. Also, the RPV thermal insulation outside the vessel is neglected due to its small neutronics effect. The detector is modeled as a cylinder hole between the vessel and the concrete.

A streaming kernel method can be devised by converting the vessel surface sources into the detector flux, as shown in Fig. 2. The vessel surface is discretized into a finite number of segments. Since the neutrons are simply streaming through the void, the Green's function from a point source (average of a vessel segment) to the detector is effectively the ratio of the solid angle that neutron can 'see' the detector over 4π. Since no transport calculation is needed outside the vessel for single kernel method, the geometry for MPACT calculation can be reduced to the right configuration (denoted as Geo_R1) in Fig. 2. The void region has been replaced by water at the jagged core boundary, so the CMFD stability issue is no more a concern, but the density of these artificial water regions should be kept constant, which is important when evaluating the detector response with perturbed moderator density.

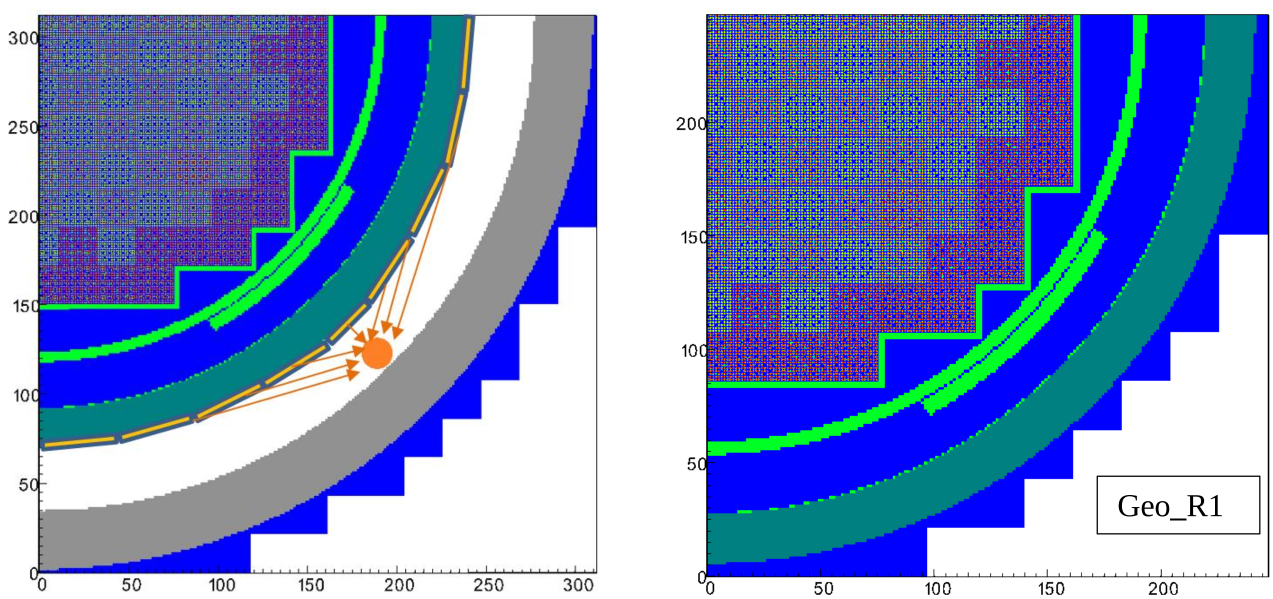

Figure 2 Illustration of neutron streaming kernel (left) and a reduced geometry for single kernel method (right)

For neutrons streaming out of the reactor vessel, the solid angle covered by the ex-core detector out of the unit sphere corresponds to the ratio that neutrons could reach the detector from the source. If the detector is assumed as a slab (the width equal to the diameter of the detector cylinder), the following figure shows $d\Omega$ with regard to the change of $d\mu$ and $d\gamma$, where μ is the cosine of polar angle θ, and γ is the azimuthal angle (see Figure 3).

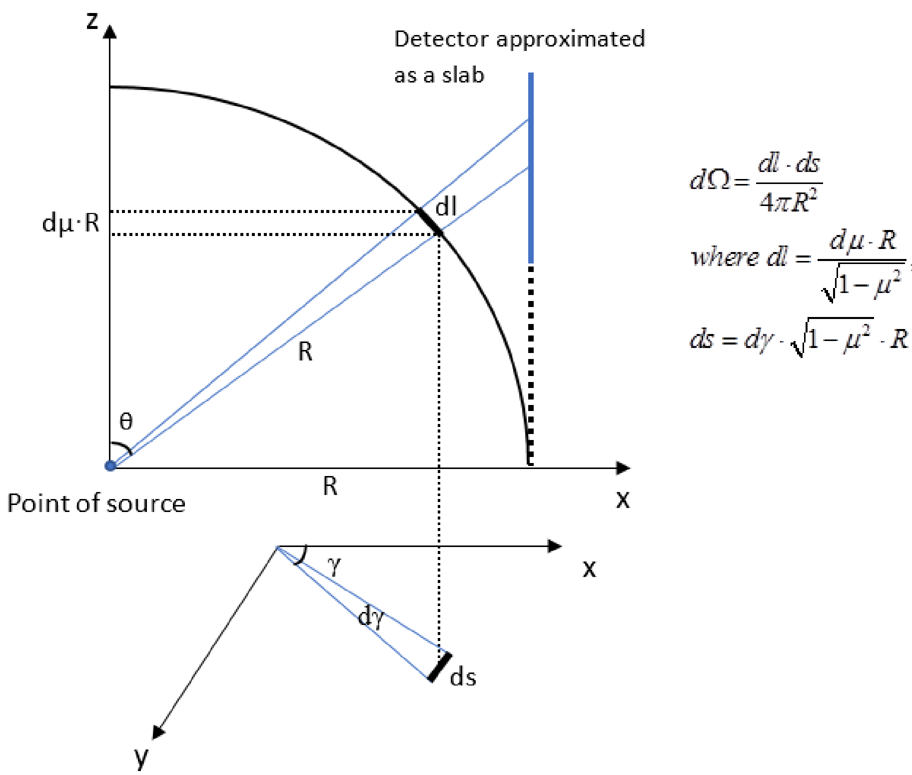

Figure 3 Solid angle covered by the detector from a point source

The ratio that neutrons emitting from the point source can reach the detector is given as,

$$S_d / S = \int_{\mu_1}^{\mu_2} \int_{\gamma_1}^{\gamma_2} \psi(\Omega) d\gamma d\mu \Big/ \int_{-1}^{1} \int_{2\pi} \psi(\Omega) d\gamma d\mu \qquad (1)$$

where $\mu_1, \mu_2, \gamma_1, \gamma_2$ can be determined by the location of source and detector and the detector size.

2.1.2 Reflector Transport Kernel

In addition to the neutron streaming kernel, the diffusion kernel was attempted in the previous milestone to further simplify the calculation and reduce the geometry. As shown in Fig. 4 (left), by selecting a surface in the reflector regions (red arc), 1-D diffusion can be solved between this surface and the outer radius of the vessel, with the boundary condition at the red surface computed from transport calculation.

However, it was identified that the accurate flux solution is obtained from the diffusion calculation only when the effective diffusion coefficients that preserve neutron current of the transport calculation are used. Porting these diffusion coefficients from CMFD calculation to the detector edits modules is found to be tedious from the code level. Therefore, a multi-group 1-D Sn solver is developed to replace the diffusion solver in this work. The Sn equation in 1D slab geometry is solved in this work,

$$\begin{aligned} &\frac{\mu_n}{h_j}(\psi_{n,j+1/2,g} - \psi_{n,j-1/2,g}) + \Sigma_{t,j,g}\psi_{n,j,g} = \frac{1}{2}\sum_{g'}\Sigma_{s,j,g'->g}\sum_{m}\psi_{m,j,g'}w_m \\ &\psi_{n,1/2,g} = \psi^{b}_{n,g} \quad (\mu_n > 0) \quad and \quad \psi_{n,J+1/2,g} = 0 \ \ (\mu_n < 0) \end{aligned} \tag{2}$$

where *j* is the spatial mesh index, *g* is the energy group index, and *m*, *n* are the quadrature indices. The incoming flux from the left boundary of the slab is obtained from MPACT transport calculation. The transport corrected P0 scattering is used. Sensitivity studies suggested that S4 with a 0.05cm spatial mesh is sufficient for the 1-D transport calculations.

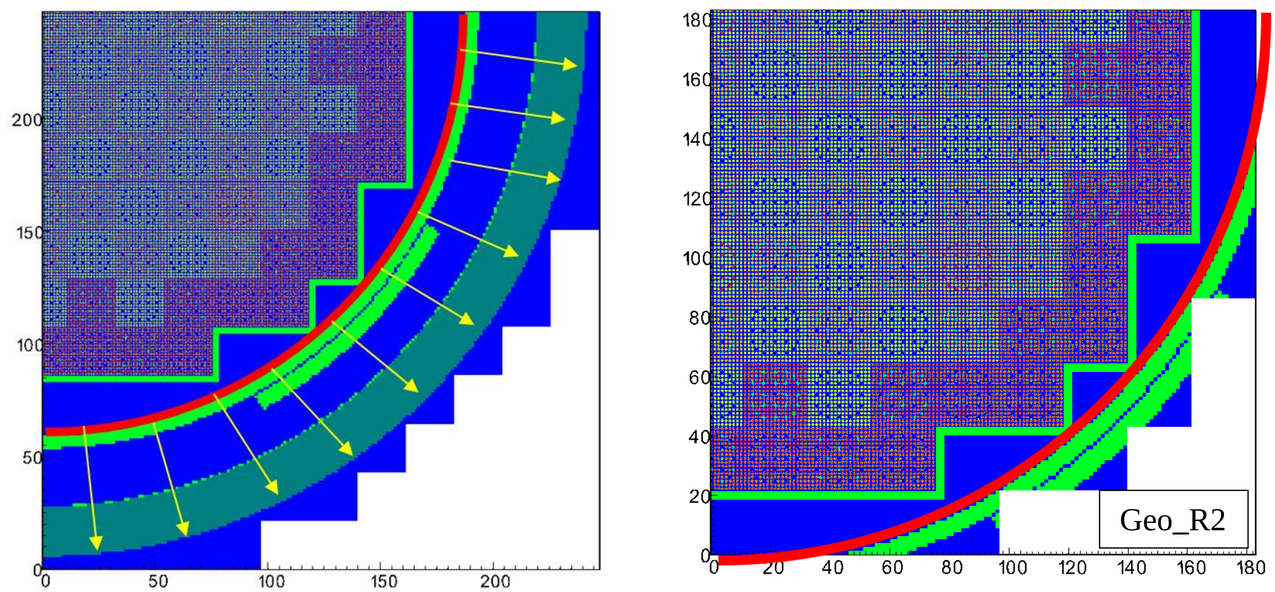

Figure 4 Illustration of 1D Sn calculation (left) and a reduced geometry for double kernel method (right)

By using the Sn solver, the MPACT transport geometry can be further reduced to Fig. 4 (right, denoted as Geo_R2). Geo_R2 is the default core geometry (one additional assembly outside the active core) in MPACT calculation. Although the Sn solver has been involved, the method still resembles the idea of ‘double kernel’ [9,10]. Therefore, the name ‘double kernel’ is still used in this work to indicate the two-step procedure. The approximations used in the double kernel method are summarized in Table 1.

Table 1 Approximations of double kernel method

Geometry Approx.	Solver Approx.
The concrete is neglected (backscattering is assumed as a constant factor)	1-D Sn solver in slab geometry is used to approximately compute the flux of the vessel outer surface
The RPV thermal insulation outside the vessel is neglected due to its small neutronics effect	The boundary conditions of Sn calculations are obtained from the transport calculation of partial reflector (one assembly outside the active core
The surveillance capsule is neglected	Assume the point source from the center of the vessel segment when calculating neutron streaming

2.2 Input Processing

The idea behind the simplified VERA inputs for ex-core detector proposed by AMA is that MPACT could directly use these inputs for simplified calculation of ex-core detector response, and Shift could use them with a default template to automatically create an omnibus input for VeraShift calculation, which saves user's efforts of diving into the full details of omnibus input.

Fig. 5 shows the proposed VERA inputs for ex-core detector. The 'vessel' card is still used to specify the reflector regions, but it has been extended up to the concrete using the 'bioshield' card. Each type of a detector is defined by its ID, geometry, material, response type, etc. The axial and radial locations of the detectors are specified in a separate card. These inputs are processed by MPACT to replace the hard-coded geometry and material information that was used in the detector response calculation routines. As long as the ex-core detectors are specified, the detector response calculation is automatically turned on.

```
[CORE]

! User defines the outer radii beyond RPV (cm)
bioshield  air         243.70
           insulation  251.70
           air_liner   258.20
           concrete    518.16

[DETECTOR]

!    ID   type       radii      / mats    / heights      / response_type [well_type]
! -------------------------------------------------------------------------------------
det  PWR  power   8.75    9.5  / air cs / 152.4 152.4 / u235   wedge
det  SRC  source  7.0612  8.89 / air cs / 148.0       / b10    none

!              ID,  radius, degree, elevation
! ---------------------------------------------
det_locations  PWR   294.2    45   42.431
               PWR   294.2   135   42.431
               PWR   294.2   225   42.431
               PWR   294.2   315   42.431
               SRC   208.1    90   83.071
               SRC   208.1   270   83.071

! all degrees are clockwise from the top of the SE quadrant. (45=SE, 135=SW)
! elevations are the distance from the bottom core plate to the bottom of the detector, in cm
! detector can be defined with multiple radii rings and multiple axial divisions (avoiding the use of axial card)
```

Figure 5 VERA inputs for ex-core detector proposed by AMA

2.3 SCRAM Signal from Excore Detector

MPACT has the capability to simulate a SCRAM scenario based on user-specified trip conditions related to core power or simulation time during a transient simulation. To facilitate the addition of SCRAM-related functionality, several input card options have been added in the previous RIA milestone [11]. However, the threshold power or power rate to trip the core was determined by the thermal power integrated over the entire core. To be consistent with plant operation, the logic of determining the core trip through ex-core detector readings is enabled. The following two input cards are related to this logic.

1. trip_power: Power threshold for SCRAM initiation.
   - trip_power <high power> <low power> <delay> <# detectors>
     i. high power: Upper core power threshold (% full power) for trip. Value must be >0.
     ii. low power: Lower core power threshold (% full power) for trip. Value must be >0.
     iii. delay: Time (sec) to defer SCRAM after trip requirements are met. Value must be ≥0.
     iv. **# detectors**: Required number of ex-core detectors reporting trip conditions for trip to occur. Values are 0 through 4. For 0, the nominal core power is used.
2. trip_rate: Power change rate threshold for SCRAM initiation.
   - trip_rate <power inc. rate> <power dec. rate> <delay> <# detectors>
     i. power inc. rate: Power rate change upper bound (% full power/sec) for trip. If the power increase rate is greater than this value, the core will trip. Negative or positive floating-point numbers are accepted.
     ii. power dec. rate: Power rate change lower bound (% full power/sec) for trip. If the power drop rate is less than this value, the core will trip. Negative or positive floating-point numbers are accepted.
     iii. delay: Time (sec) to defer SCRAM after trip requirements are met. Value must be ≥0.
     iv. **# detectors**: Required number of ex-core detectors reporting trip conditions for trip to occur. Values are 0 through 4. For 0, the nominal core power is used.

When user specifies the number of ex-core detectors to be used for trip to occur, MPACT will look through the history of detector readings and compute the relative power or power rate for each ex-core detector. When the number of detectors that meet the power or power rate criterion is larger than the number of detectors (# detectors) specified in the input, the trip is triggered. If 0 is used, the nominal power integrated over the core is still used.

3. NUMERICAL RESULTS

The detector response models in Section 2 are verified with VeraShift calculations. The test problem is a WBN1 quarter core at BOL and HZP (Problem 5a). The Shift model was run with full ex-core geometry as shown in Fig. 1. The moderator density is perturbed uniformly (including downcomer) from 0.6g/cc to 0.8g/cc to effectively change the neutron spectrum and its leakage out of the vessel. The total detector response (sum of upper and lower detectors) are tallied in the Shift runs. This test should be able to verify if the Sn and neutron streaming solvers in MPACT could properly model the neutron attenuation and leakage through the reflector. Fig. 6 shows the relative detector responses between VERA-Shift and the double kernel method from MPACT. The results are normalized to unity at 0.6g/cc. The relative responses from MPACT are within 2-sigma error of VeraShift. Since the VeraShift results were run without CADIS for these problems, the uncertainties are non-trivial.

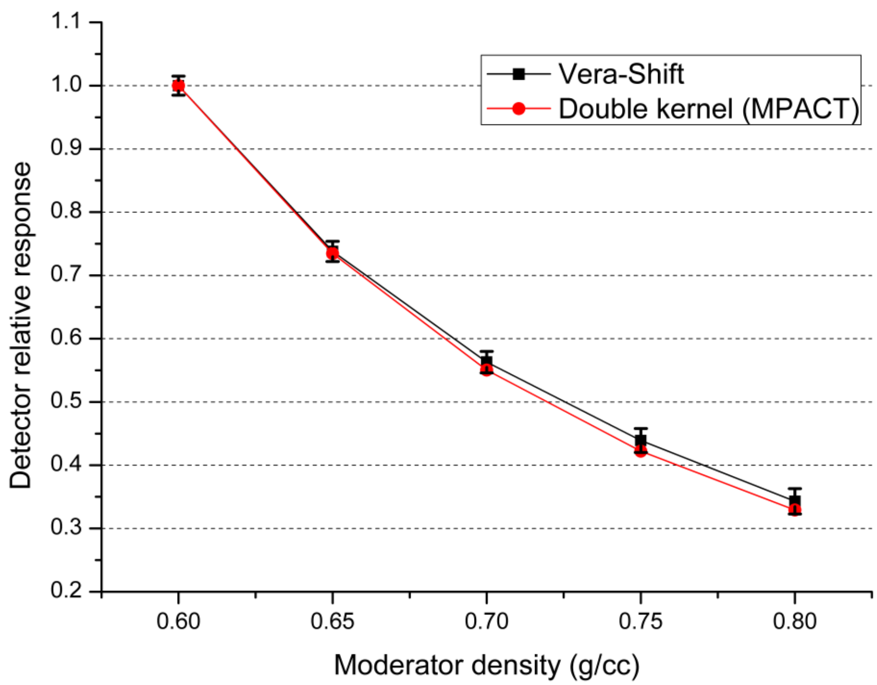

Figure 6 Comparison of relative detector response vs moderator density

A second comparison was performed to verify the axial effect on detector response. Several P5 cases were run with different control rod positions of Bank D, and the bottom and top detector responses are tallied separately. Instead of comparing the detector responses, it is more interesting to compare the axial offset (AO),

$$AO = \frac{R_{top} - R_{bot}}{R_{top} + R_{bot}} \tag{3}$$

where R_{top} and R_{bot} are the responses of top and bottom detectors. In Fig. 7, the AOs computed by detector responses from MPACT and VeraShift are also compared with that computed by top and bottom core powers from MPACT. There are two missing points for the VeraShift results, where we are still investigating the issue of running these two rod positions. But for the rest three rod positions, the AOs from MPACT agree with VeraShift within 2% of AO. The uncertainties of VeraShift results are much smaller (less than 0.05%) since CADIS was used in these calculations. The AOs computed from the integrated top and bottom core powers are largely different from the detector AOs since only the peripheral assemblies are important for ex-core detector response.

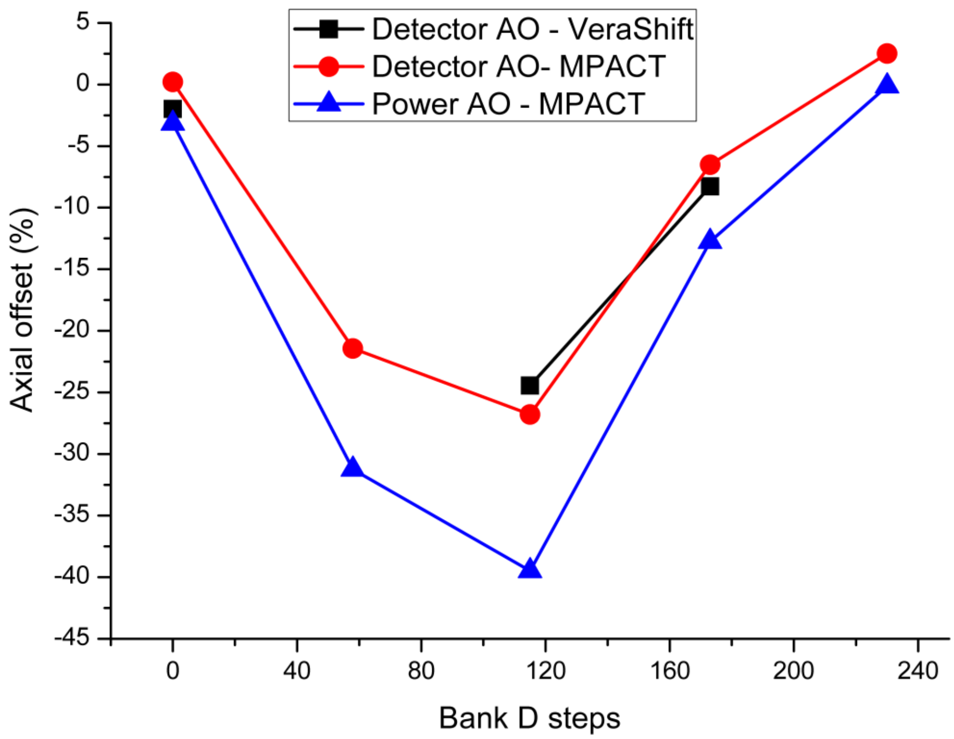

Figure 7 The axial offset vs Bank D position

Table 2 shows the computational resources for the double kernel method. Since the calculation is based on the default MPACT geometry (Geo_R2 in Fig. 4), the computation efforts of MPACT transport calculation is unchanged. The only extra calculations are the 1-D Sn transport for the discretized segments in the reflector, and the simple streaming calculation from vessel to detector. The overall computing time increases less than 1% for all the Problem 5 cases we tested.

Table 2 Additional computing resources

Item	Double kernel
Additional memory	Trivial
Geometry model	Geo_R2 (default)
Additional time	Less than 1.0%

The SCRAM logic using ex-core detector signals are also tested by comparing it to the logic using integrated core power. A mini core of 3x3 assemblies with ex-core geometry is mocked up to run a transient of rod ejection. Table 3 shows a comparison of integrated core power and relative detector signals during a rod ejection followed by a SCRAM. For both cases, the criterion to trip the core is >120% power (a delay of 0.02s is specified for mechanism to kick in). Both cases trigger SCRAM at State 4, and the rods start to be inserted back after State 8. The relative power from integrated core power and detector readings are somewhat different over the transient, which is expected.

Table 3 Comparison of using integrated power and detector readings for SCRAM

State	Time(s)	Reactivity($)	Relative power from integrated core power	Relative power from ex-core detector readings
1	0	0	100.0	100.0
2	0.005	0.1539	101.9	101.0
3	0.01	0.3844	118.7	115.5
4	**0.015**	**0.7189**	**156.7**	**148.6**
5	0.02	1.1601	255.4	234.8
6	0.025	1.6790	597.6	534.2
7	0.03	2.2069	2504.9	2202.2
8	**0.035**	**2.6559**	**19965.0**	**17540.0**
9	0.04	1.3946	67630.5	59797.2
10	0.045	-0.9975	3059.5	2794.2
11	0.05	-1.5074	172.3	161.9
12	0.055	-1.9000	101.1	97.2
13	0.06	-2.2008	89.7	87.9
14	0.065	-2.4150	83.1	82.5
15	0.07	-2.5604	78.9	79.0
16	0.075	-2.5532	78.3	78.5
17	0.08	-2.5467	78.1	78.2
18	0.085	-2.5401	77.9	78.0
19	0.09	-2.5336	77.6	77.8
20	0.095	-2.5272	77.4	77.6
21	0.1	-2.5208	77.2	77.3
22	0.12	-2.5092	76.0	76.2
23	0.14	-2.4846	75.2	75.3
24	0.16	-2.4607	74.3	74.5
25	0.18	-2.4377	73.5	73.7
26	0.2	-2.4154	72.8	73.0

4. SUMMARY AND FUTURE ACTIVITIES

The ex-core detector response calculation model has been successfully integrated into MPACT. The double kernel method is chosen because it could run with the default MPACT geometry (no extensive modeling of full reflector and vessel regions). To overcome the difficulty of obtaining the consistent diffusion coefficients, the 1-D diffusion solver is replaced by a 1-D Sn transport solver in the double kernel method. Although the double kernel method uses several approximations such as low-order solvers and simplified ex-core and detector geometries, the detector responses from MPACT compares reasonably good with VeraShift calculation. The detector signals are linked to the SCRAM logic as an option to trip the core during transient calculations.

The ongoing work is to implement the axial offset edits into the summary file, which is recently requested by AMA. This should be done consistently between MPACT and VeraShift so that a uniform output format is expected no matter which option is used for the ex-core detector response calculation. Also, additional problems are needed to run between MPACT and VeraShift for further comparisons.

REFERENCES

1. J. A. Turner et al., "The Virtual Environment for Reactor Applications (VERA): Design and architecture," *Journal of Computational Physics*, **326**, 544 (2016).
2. T. M. Pandya, T. Evans, K. Clarno, and B. Collins, Ex-core Radiation Transport Modeling with VERA: Manual, Consortium for Advanced Simulation of LWRs (CASL), CASL-U-2018-1556-000 (2018).
3. E. Davidson, T. Pandya, A. Godfrey, T. Evans, "Testing of Omnibus General Geometry Models for Ex-Core Applications in VERA," Consortium for Advanced Simulation of LWRs (CASL), CASL-U-2018-1561-000 (2018).
4. MPACT Team, "MPACT: User's Manual Version 1.0.0", November 8, 2013.
5. T. M. Pandya, S. R. Johnson, T. M. Evans, G. G. Davidson, S. P. Hamilton, and A. T. Godfrey, "Capabilities, Implementation, and Benchmarking of Shift, a Massively Parallel Monte Carlo Radiation Transport Code," *Journal of Computational Physics*, **308**, 239 (2016).
6. Y. Liu and E. Davidson, "Development of Simplified Methods for Ex-core Detector Response in MPACT," CASL-U-2018-1699-001 (2018).
7. Westinghouse Technology Systems Manual, Section 9.1: Excore Nuclear Instrumentation.
8. M. W. Crump and J. C. Lee, "Calculation of Spatial Weighting Functions for Ex-Core Neutron Detectors," *Nuclear Technology*, **41**, 87-96 (1978).
9. H. Tochihara, E. Ochiai, T. Hasegawa, "Reevaluation of Spatial Weighting Factors for Ex-Core Neutron Detectors," *Nuclear Technology*, **58**, 310-317 (1982).
10. T. Bahadir, M. Giffen and C. Wells, "Fixed-Source and Ex-core Detector Calculations with SIMULATE5," *M&C 2017*, Jeju, Korea, April 16-20 (2017).
11. B. Kochunas, Y. Liu, D. Jabaay, Z. Dodson, Q. Shen, A. Gerlach, A. Wysocki, "MPACT RIA Transient Modeling," CASL-U-2018-1544-000, March 31, 2018.